J|A|C|S ARTICLES

Published on Web 03/13/2009

Double Helix Formation of Oligoresorcinols in Water: Thermodynamic and Kinetic Aspects

Hidetoshi Goto,[†] Yoshio Furusho,*[,†,‡] Kazuhiro Miwa,[†,‡] and Eiji Yashima*[,†,‡]

Yashima Super-structured Helix Project, Exploratory Research for Advanced Technology (ERATO), Japan Science and Technology Agency (JST), Japan, and Department of Molecular Design and Engineering, Graduate School of Engineering, Nagoya University, Chikusa-ku, Nagoya 464-8603, Japan

Received November 1, 2008; E-mail: furusho@apchem.nagoya-u.ac.jp; yashima@apchem.nagoya-u.ac.jp

Abstract: We previously reported that the oligoresorcinols formed double-stranded helices in neutral water through interstrand aromatic interactions. In the present study, we synthesized a new series of oligomers from the 2mer to the 15mer to explore the thermodynamics, kinetics, and mechanism of the double helix formation of the oligoresorcinols in water. The double helix formation was dependent on the chain length of the oligomers and significantly affected by solvent, pH, salt, and temperature. The free energy change ($-\Delta G$) for the double helix formation linearly increased with the chain length from the 4mer to the 11mer ($\Delta\Delta G = -0.94$ kcal mol^{-1} unit^{-1}), whereas it did not change for the oligomers longer than the 11mer. The van't Hoff analysis of the 9mer revealed that the double helix formation was an enthalpically driven process ($\Delta H = -27 \pm 1.5$ kcal mol^{-1} and $\Delta S = -70 \pm 5$ cal mol^{-1} K^{-1}), which was consistent with the upfield shifts in the ^{1}H NMR spectra and the hypochromicity of the absorption spectra as a result of the interstrand aromatic interactions in water. Furthermore, the kinetic analysis of the chain exchange reaction between the double helices of the optically active and optically inactive 11mers revealed a small $\Delta S^{\ddagger}$, suggesting that the chain exchange proceeds not via the dissociation−association pathway, but via the direct exchange pathway.

Introduction

Biomacromolecules, such as proteins and DNA, adopt a one-handed helical conformation that is essential and indispensable for biological functions, thereby having prompted chemists to develop artificial oligomers and polymers with a helical conformation. Whereas a number of oligomers and polymers that fold into a single helical conformation have been reported to date,[1,2] the synthetic design of artificial double helices remains a challenging task,[2−9] since one needs to take into account not only the chemical structure of the strands, but also the interstrand interactions that drive the two molecular strands to intertwine each other. Metal coordination has been most widely used for the construction of double-stranded metal complexes (i.e., helicates).[4] Although hydrogen bonding has been extensively employed for the design of supramolecular duplexes,[10] most of their three-dimensional structures are characterized as not helical but ladder- or zipperlike linear conformations.[11,12] Some aromatic oligoamides have been reported to fold into double helices through hydrogen bonding as well as aromatic stacking interactions,[5] and hydrogen bonding-driven self-assembly with anion templates has been used to construct double helices.[6] Recently, we designed and synthesized a series of heterostranded double helices with a controlled helix sense consisting of molecular strands complementary to each other, utilizing

[†] ERATO, JST.
[‡] Nagoya University.

(1) For reviews on synthetic polymers and oligomers with single helical conformations, see: (a) Rowan, A. E.; Nolte, R. J. M. *Angew. Chem., Int. Ed.* **1998**, *37*, 63–68. (b) Gellman, S. H. *Acc. Chem. Soc.* **1998**, *31*, 173–180. (c) Green, M. M.; Park, J.-W.; Sato, T.; Teramoto, A.; Lifson, S.; Selinger, R. L. B.; Selinger, J. V. *Angew. Chem., Int. Ed.* **1999**, *38*, 3138–3154. (d) Nakano, T.; Okamoto, Y. *Chem. Rev.* **2001**, *101*, 4013–4038. (e) Hill, D. J.; Mio, M. J.; Prince, R. B.; Hughes, T. S.; Moore, J. S. *Chem. Rev.* **2001**, *101*, 3893–4011. (f) Cornelissen, J. J. L. M.; Rowan, A. E.; Nolte, R. J. M.; Sommerdijk, N. A. J. M. *Chem. Rev.* **2001**, *101*, 4039–4070. (g) Brunsveld, L.; Folmer, B. J. B.; Meijer, E. W.; Sijbesma, R. P. *Chem. Rev.* **2001**, *101*, 4071–4097. (h) Nomura, R.; Nakako, H.; Masuda, T. *J. Mol. Catal. A: Chem.* **2002**, *190*, 197–205. (i) Fujiki, M. *J. Organomet. Chem.* **2003**, *685*, 15–34. (j) Yashima, E.; Maeda, K.; Nishimura, T. *Chem.—Eur. J.* **2004**, *10*, 42–51. (k) Lam, J. W. Y.; Tang, B. Z. *Acc. Chem. Res.* **2005**, *38*, 745–754. (l) Maeda, K.; Yashima, E. *Top. Curr. Chem.* **2006**, *265*, 47–88. (m) Stone, M. T.; Heemstra, J. M.; Moore, J. S. *Acc. Chem. Res.* **2006**, *39*, 11–20. (n) Pijper, D.; Feringa, B. L. *Soft Matter* **2008**, *4*, 1349–1372. (o) Yashima, E.; Maeda, K. *Macromolecules* **2008**, *41*, 3–12.

(2) *Foldamers: Structure, Properties, and Applications*; Hecht, S., Huc, I., Eds.; Wiley-VCH: Weinheim, Germany, 2007.

(3) For reviews on synthetic double helices, see: (a) Lehn, J.-M. *Supramolecular Chemistry: Concepts and Perspectives*; VCH: Weinheim, Germany, 1995. (b) Nielsen, P. E. *Acc. Chem. Res.* **1999**, *32*, 624–630. (c) Albrecht, M. *Chem. Rev.* **2001**, *101*, 3457–3497. (d) Huc, I. *Eur. J. Org. Chem.* **2004**, 17–29. (e) Albrecht, M. *Angew. Chem., Int. Ed.* **2005**, *44*, 6448–6451. (f) Furusho, Y.; Yashima, E. *Chem. Rec.* **2007**, *7*, 1–11. (g) Amemiya, R.; Yamaguchi, M. *Chem. Rec.* **2008**, *8*, 116–127.

(4) For examples of helicates, see: (a) Lehn, J.-M.; Rigault, A.; Siegel, J.; Harrowfield, J.; Chevrier, B.; Moras, D. *Proc. Natl. Acad. Sci. U.S.A.* **1987**, *84*, 2565–2569. (b) Koert, U.; Harding, M. M.; Lehn, J.-M. *Nature* **1990**, *346*, 339–342. (c) Woods, C. R.; Benaglia, M.; Cozzi, F.; Siegel, J. S. *Angew. Chem., Int. Ed. Engl.* **1996**, *35*, 1830–1833. (d) Orita, A.; Nakano, T.; An, D. L.; Tanikawa, K.; Wakamatsu, K.; Otera, J. *J. Am. Chem. Soc.* **2004**, *126*, 10389–10396. (e) Katagiri, H.; Miyagawa, T.; Furusho, Y.; Yashima, E. *Angew. Chem., Int. Ed.* **2006**, *45*, 1741–1744.

 10.1021/ja808585y CCC: $40.75

amidinium-carboxylate salt bridges that have a high stability and well-defined directionality.[7]

On the other hand, water-soluble helical oligomers and polymers are quite few,[13] although they have attracted considerable attention, since important biological events occur in water, where most biomacromolecules adopt a helical conformation. Therefore, the design and synthesis of water-soluble artificial double helices based on noncovalent interactions represent a special challenge despite the recent development in supramolecular chemistry. During the course of our studies on developing water-soluble, single helical foldamers based on the oligo- and poly-*m*-phenylenes that are known to form a 5_1-helical conformation in the solid state,[14] we serendipitously found that the oligoresorcinols self-assembled into well-defined double-stranded helical structures in water through interstrand aromatic interactions (Figure 1).[9] The oligoresorcinols showed a high affinity and selectivity toward oligosaccharides in water, hence forming heterodouble helices and [3]pseudorotaxanes with the *linear* and *cyclic* oligosaccharides, respectively.[9b,c]

In the present study, we synthesized a series of discrete chiral and/or achiral oligoresorcinols from 2mer to 15mer and systematically investigated the effects of solvents, chiral side chains, temperature, salts, and pH together with the chain length dependence on the double helix formation of the oligoresorcinols in water with the aim of exploring the mechanism of the double helix formation at a molecular level. Chain-length dependence tests were employed and provide valuable information on the structural and physicochemical features of macromolecular and

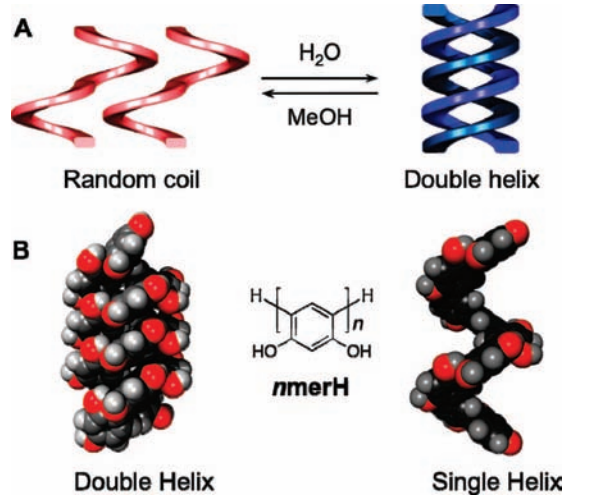

Figure 1. (A) Schematic illustration of double helix formation of oligoresorcinols. (B) Molecular mechanics calculated structures of the double helix and the single strand of **9merH** ($n = 9$).[9a]

foldamer systems.[1m] However, only one example has been reported for synthetic double helices,[5c] as opposed to thoroughly studied single-stranded helical foldamers, such as oligo(*m*-phenyleneethynylene)s.[1m] In addition, we investigated the thermodynamic and kinetic stabilities of the oligoresorcinol double helices by determining the association constants for the double helix formation and the rates for the chain exchange between the double helices of the optically active and optically inactive oligoresorcinols in water, respectively. The kinetics of double helix formation is of particular interest, because it would give insight into the mechanistic details. However, to the best of our knowledge, there has been no report on kinetics on the chain exchange process during the double helix formation, except for the seminal example of aromatic oligoamide-based double helices investigated by molecular dynamics simulations.[5b]

The present results reported herein will contribute to a fundamental understanding of the mechanisms and interstrand interactions of double helix formations of biological and artificial

(5) For examples of aromatic oligoamides that fold into double helices, see: (a) Berl, V.; Huc, I.; Khoury, R. G.; Krische, M. J.; Lehn, J.-M. *Nature* **2000**, *407*, 720–723. (b) Berl, V.; Huc, I.; Khoury, R. G.; Lehn, J.-M. *Chem.—Eur. J.* **2001**, *7*, 2810–2820. (c) Jiang, H.; Maurizot, V.; Huc, I. *Tetrahedron* **2004**, *60*, 10029–10038. (d) Maurizot, V.; Dolain, C.; Huc, I. *Eur. J. Org. Chem.* **2005**, 1293–1301. (e) Dolain, C.; Zhan, C.; Leger, J.-M.; Daniels, L.; Huc, I. *J. Am. Chem. Soc.* **2005**, *127*, 2400–2401. (f) Zhan, C.; Leger, J.-M.; Huc, I. *Angew. Chem., Int. Ed.* **2006**, *45*, 4625–4628. (g) Haldar, D.; Jiang, H.; Leger, J.-M.; Huc, I. *Angew. Chem., Int. Ed.* **2006**, *45*, 5483–5486. (h) Berni, E.; Kauffmann, B.; Bao, C.; Lefeuvre, J.; Bassani, D. M.; Huc, I. *Chem.—Eur. J.* **2007**, *13*, 8463–8469. (i) Gan, Q.; Bao, C.; Kauffmann, B.; Grelard, A.; Xiang, J.; Liu, S.; Huc, I.; Jiang, H. *Angew. Chem., Int. Ed.* **2008**, *47*, 1715–1718. (j) Berni, E.; Garric, J.; Lamit, C.; Kauffmann, B.; Leger, J.-M.; Huc, I. *Chem. Commun.* **2008**, 1968–1970.

(6) For examples of anion-templated double helices, see: (a) Sánchez-Quesada, J.; Seel, C.; Prados, P.; de Mendoza, J. *J. Am. Chem. Soc.* **1996**, *118*, 277–278. (b) Keegan, J.; Kruger, P. E.; Nieuwenhuyzen, M.; O'Brien, J.; Martin, N. *Chem. Commun.* **2001**, 2192–2193. (c) Coles, S. J.; Frey, J. G.; Gale, P. A.; Hursthouse, M. B.; Light, M. E.; Navakhun, K.; Thomas, G. L. *Chem. Commun.* **2003**, 568–569.

(7) For artificial double helices based on amidinium-carboxylate salt bridges, see: (a) Tanaka, Y.; Katagiri, H.; Furusho, Y.; Yashima, E. *Angew. Chem., Int. Ed.* **2005**, *44*, 3867–3870. (b) Ikeda, M.; Tanaka, Y.; Hasegawa, T.; Furusho, Y.; Yashima, E. *J. Am. Chem. Soc.* **2006**, *128*, 6806–6807. (c) Furusho, Y.; Tanaka, Y.; Yashima, E. *Org. Lett.* **2006**, *8*, 2583–2586. (d) Furusho, Y.; Tanaka, Y.; Maeda, T.; Ikeda, M.; Yashima, E. *Chem. Commun.* **2007**, 3174–3176. (e) Hasegawa, T.; Furusho, Y.; Katagiri, H.; Yashima, E. *Angew. Chem., Int. Ed.* **2007**, *46*, 5885–5888. (f) Maeda, T.; Furusho, Y.; Sakurai, S.-i.; Kumaki, J.; Okoshi, K.; Yashima, E. *J. Am. Chem. Soc.* **2008**, *130*, 7938–7945. (g) Ito, H.; Furusho, Y.; Hasegawa, T.; Yashima, E. *J. Am. Chem. Soc.* **2008**, *130*, 14008–14015.

(8) For helicene-based double helices, see: (a) Sugiura, H.; Nigorikawa, Y.; Saiki, Y.; Nakamura, K.; Yamaguchi, M. *J. Am. Chem. Soc.* **2004**, *126*, 14858–14864. (b) Sugiura, H.; Yamaguchi, M. *Chem. Lett.* **2007**, *36*, 58–59. (c) Sugiura, H.; Amemiya, R.; Yamaguchi, M. *Chem.—Asian J.* **2008**, *3*, 244–260.

(9) For oligoresorcinol-based double helices, see: (a) Goto, H.; Katagiri, H.; Furusho, Y.; Yashima, E. *J. Am. Chem. Soc.* **2006**, *128*, 7176–7178. (b) Goto, H.; Furusho, Y.; Yashima, E. *J. Am. Chem. Soc.* **2007**, *129*, 109–112. (c) Goto, H.; Furusho, Y.; Yashima, E. *J. Am. Chem. Soc.* **2007**, *129*, 9168–9174.

(10) For a review on hydrogen bonding-driven duplex formation, see: Prins, L. J.; Reinhoudt, D. N.; Timmerman, P. *Angew. Chem., Int. Ed.* **2001**, *40*, 2382–2426.

(11) For examples of hydrogen bonding-driven duplexes based on oligoamides, see: (a) Gong, B.; Yan, Y.; Zeng, H.; Skrzypczak-Jankunn, E.; Kim, Y. W.; Zhu, J.; Ickes, H. *J. Am. Chem. Soc.* **1999**, *121*, 5607–5608. (b) Nowick, J. S.; Chung, D. M.; Maitra, K.; Maitra, S.; Stigers, K. D.; Sun, Y. *J. Am. Chem. Soc.* **2000**, *122*, 7654–7661. (c) Bisson, A. P.; Carver, F. J.; Eggleston, D. S.; Haltiwanger, R. C.; Hunter, C. A.; Livingstone, D. L.; McCabe, J. F.; Rotger, C.; Rowan, A. E. *J. Am. Chem. Soc.* **2000**, *122*, 8856–8868. (d) Zeng, H.; Yang, X.; Flowers, R. A.; Gong, B. *J. Am. Chem. Soc.* **2002**, *124*, 2903–2910. (e) Moriuchi, T.; Tamura, T.; Hirao, T. *J. Am. Chem. Soc.* **2002**, *124*, 9356–9357. (f) Yang, X.; Martinovic, S.; Smith, R. D.; Gong, B. *J. Am. Chem. Soc.* **2003**, *125*, 9932–9933. (g) Yang, X.; Gong, B. *Angew. Chem., Int. Ed.* **2005**, *44*, 1352–1356.

(12) For examples of hydrogen bonding-driven duplexes based on heterocycles, see: (a) Sessler, J. L.; Wang, R. *J. Am. Chem. Soc.* **1996**, *118*, 9808–9809. (b) Folmer, B. J. B.; Sijbesma, R. P.; Kooijman, H.; Spek, A. L.; Meijer, E. W. *J. Am. Chem. Soc.* **1999**, *121*, 9001–9007. (c) Corbin, P. S.; Zimmerman, S. C. *J. Am. Chem. Soc.* **2000**, *122*, 3779–3780. (d) Archer, E. A.; Goldberg, N. T.; Lynch, V.; Krische, M. J. *J. Am. Chem. Soc.* **2000**, *122*, 5006–5007. (e) Corbin, P. S.; Zimmerman, S. C.; Thiessen, P. A.; Hawryluk, N. A.; Murray, T. J. *J. Am. Chem. Soc.* **2001**, *123*, 10475–10488. (f) Gong, H.; Krische, M. J. *J. Am. Chem. Soc.* **2005**, *127*, 1719–1725.

double helices and also provide the rationale for molecular design of artificial double helices with specific functions.

Results and Discussion

Synthesis of Oligoresorcinols. Polyphenols are known to be prepared by the oxidative coupling polymerization of phenols.[15] However, during the oxidative coupling oligo- or polymerization of unprotected phenols, controlling the regioselectivity is often very difficult, hence producing polyphenols consisting of a mixture of phenylene (CC) and oxyphenylene (CO) units due to the side C−O coupling. Therefore, a stepwise synthetic protocol was required for preparing oligophenols with a well-defined structure.[16] We then synthesized a series of optically inactive oligoresorcinols from 2mer to 15mer in a stepwise manner, as shown in Scheme 1.[9a] The *O*-methyl-protected oligoresorcinols (**2merMe**−**12merMe** and **15merMe**) were prepared by the repetitive Suzuki coupling of the appropriate bromides and boronates by starting from the 1,3-dimethoxybenzene (**1merMe**). Finally, a series of oligoresorcinols with different chain lengths (**2merH**−**12merH** and **15merH**) were obtained by the deprotection of the corresponding *O*-methyl-protected oligomers with BBr_3 in moderate yields. All oligoresorcinols were characterized by ^{1}H-, ^{13}C NMR, and IR spectroscopies and mass spectrometry (see Supporting Information).

The double helices of the oligoresorcinols formed in aqueous solution exist as equimolar mixtures of the right- and left-handed forms, that is, racemates. With the aim of biasing the helix sense

Scheme 1. Synthesis of the Oligoresorcinols (**2merH**−**12merH** and **15merH**)[a]

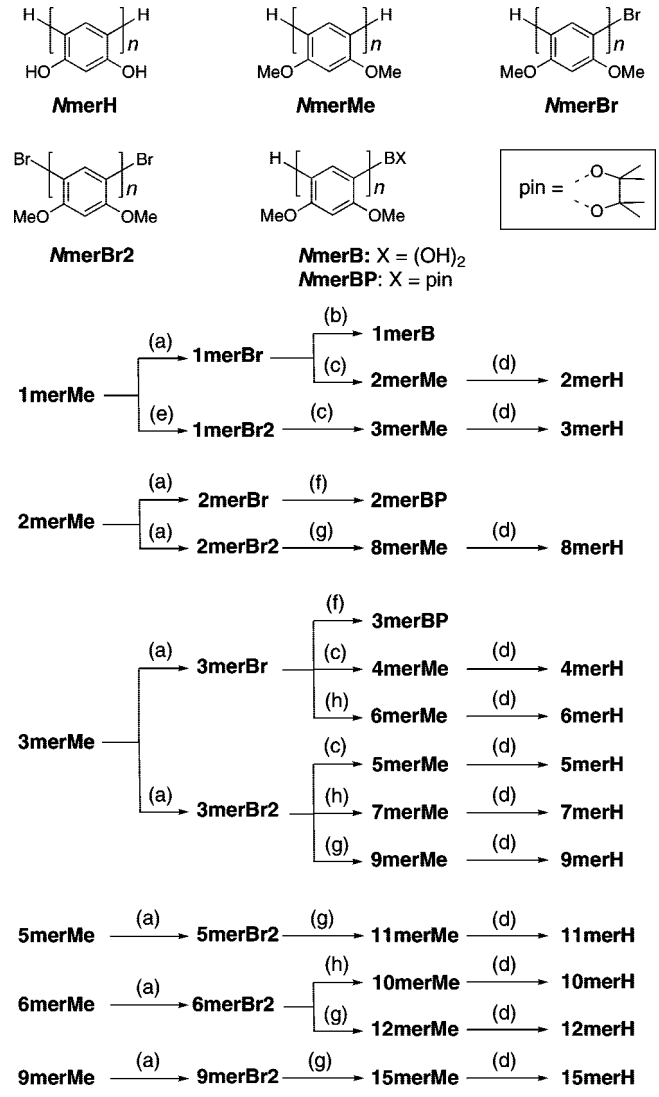

[a] Reagents and conditions: (a) 1,3-dibromo-5,5-dimethylhydantoin (DBH), THF, 0 °C, 1 day; (b) (i) *n*-BuLi, THF, −78 °C, 1 h, (ii) B(O*i*-Pr)$_3$, −78 °C, 1 day, (iii) H_3O^+; (c) **1merB**, $Pd(PPh_3)_4$, K_2CO_3, THF, H_2O, reflux, 3 days; (d) (i) BBr_3, 0 °C, 1 day, (ii) H_2O; (e) HBr, DMSO, reflux, 1 day; (f) pinacolborane, $PdCl_2(PPh_3)_2$, Et_3N, 1,4-dioxane, 80 °C, 1 day; (g) **3merBP**, $Pd(PPh_3)_4$, K_2CO_3, toluene, H_2O, 80 °C, 3 days; (h) **2merBP**, $Pd(PPh_3)_4$, K_2CO_3, toluene, H_2O, 80 °C, 3 days.

of the double helices, we designed and synthesized the oligoresorcinols with chiral side chains at both ends of the strands (**8merHR2** and **11merHR2**) (Scheme 2).[9a,17] We chose the commercially available (*S*)-1-bromo-2-methylbutane with a high enantiomeric purity as the starting material of the side chain, which introduces a chiral center in close proximity to the aromatic backbone. In addition, it lacks absorption in the oligoresorcinol region above 200 nm, thereby facilitating the absorption and CD spectral studies. The chiral side chain

(13) For examples of water-soluble helical polymers and oligomers, see: (a) Wittung, P.; Eriksson, M.; Lyng, R.; Nielsen, P. E.; Nordén, B. *J. Am. Chem. Soc.* **1995**, *117*, 10167–10173. (b) Seebach, D.; Overhand, M.; Kühnle, F. N. M.; Martinoni, B.; Oberer, L.; Hommel, U.; Widmer, H. *Helv. Chim. Acta* **1996**, *79*, 913–941. (c) Appella, D. H.; Christianson, L. A.; Karle, I. L.; Powell, D. R.; Gellman, S. H. *J. Am. Chem. Soc.* **1996**, *118*, 13071–13072. (d) Onouchi, H.; Maeda, K.; Yashima, E. *J. Am. Chem. Soc.* **2001**, *123*, 7441–7442. (e) Cornelissen, J. J. L. M.; Donners, J. J. J. M.; de Gelder, R.; Graswinckel, W. S.; Metselaar, G. A.; Rowan, A. E.; Sommerdijk, N. A. J. M.; Nolte, R. J. M. *Science* **2001**, *293*, 676–680. (f) Ishikawa, M.; Maeda, K.; Mitsutsuji, Y.; Yashima, E. *J. Am. Chem. Soc.* **2004**, *126*, 732–733. (g) Maeda, K.; Ishikawa, M.; Yashima, E. *J. Am. Chem. Soc.* **2004**, *126*, 15161–15166. (h) Arnt, L.; Tew, G. N. *Macromolecules* **2004**, *37*, 1283–1288. (i) Tan, C.; Pinto, M. R.; Kose, M. E.; Ghiviriga, I.; Schanze, K. S. *Adv. Mater.* **2004**, *16*, 1208–1212. (j) Sinkeldam, R. W.; van Houtem, M. H. C. J.; Pieterse, K.; Vekemans, J. A. J. M.; Meijer, E. W. *Chem.−Eur. J.* **2006**, *12*, 6129–6137. (k) Waki, M.; Abe, H.; Inouye, M. *Chem.−Eur. J.* **2006**, *12*, 7639–7647. (l) Waki, M.; Abe, H.; Inouye, M. *Angew. Chem., Int. Ed.* **2007**, *46*, 3059–3061. (m) Gillies, E. R.; Deiss, F.; Staedel, C.; Schmitter, J.-M.; Huc, I. *Angew. Chem., Int. Ed.* **2007**, *46*, 4081–4084.

(14) (a) Williams, D. J.; Colquhoun, H. M.; O'Mahoney, C. A. *J. Chem. Soc., Chem. Commun.* **1994**, 1643–1644. (b) Colquhoun, H. M.; Williams, D. J. *Acc. Chem. Res.* **2000**, *33*, 189–198. (c) Kobayashi, N.; Sasaki, S.; Abe, M.; Watanabe, S.; Fukumoto, H.; Yamamoto, T. *Macromolecules* **2004**, *37*, 7986–7991.

(15) For recent reviews and articles on the polymerization of phenols, see: (a) Reihmann, M. H.; Ritter, H. *Macromol. Chem. Phys.* **2000**, *201*, 798–804. (b) Fukuoka, T.; Tachibana, Y.; Tonami, H.; Uyama, H.; Kobayashi, S. *Biomacromolecules* **2002**, *3*, 768–774. (c) Xu, P.; Kumar, J.; Samuelson, L.; Cholli, A. L. *Biomacromolecules* **2002**, *3*, 889–893. (d) Kim, Y.-J.; Uyama, H.; Kobayashi, S. *Macromolecules* **2003**, *36*, 5058–5060. (e) Kobayashi, S.; Higashimura, H. *Prog. Polym. Sci.* **2003**, *28*, 1015–1048. (f) Habaue, S.; Ohnuma, M.; Mizoe, M.; Tenma, T. *Polym. J.* **2005**, *37*, 625–628.

(16) (a) Cram, D. J.; Kaneda, T.; Helgeson, R. C.; Brown, S. B.; Knolber, C. B.; Maverick, E.; Trueblood, K. N. *J. Am. Chem. Soc.* **1985**, *107*, 3645–3657. (b) Sartori, G.; Maggi, R.; Bigi, F.; Arienti, A.; Casnati, G. *Tetrahedron* **1992**, *48*, 9483–9494. (c) Sartori, G.; Maggi, R.; Bigi, F.; Grandi, M. *J. Org. Chem.* **1994**, *59*, 3701–3703. (d) Wolbers, M. P. O.; van Veggel, F. C. J. M.; Snellink-Ruël, B. H. M.; Hofstraat, J. W.; Guerts, F. A. J.; Reinhoudt, D. N. *J. Am. Chem. Soc.* **1997**, *119*, 138–144.

(17) In our previous study (ref 9a), **11merR2** was synthesized via the Suzuki coupling of **1merRBP** and **9merBr2**. However, the crude product contained side products including the 10mer of which the polarity and the molecular size are quite similar to those of **11merHR2**, thus making the purification of **11merR2** using chromatography extremely difficult. The new synthetic route employed in the present study adopts the Suzuki coupling of **7merRI** and **4merRBP**, in which the purification was attained without much of a problem (see the Supporting Information).

Scheme 2. Synthesis of the Oligoresorcinols with Chiral Side Chains (**8merHR2** and **11merHR2**)[a]

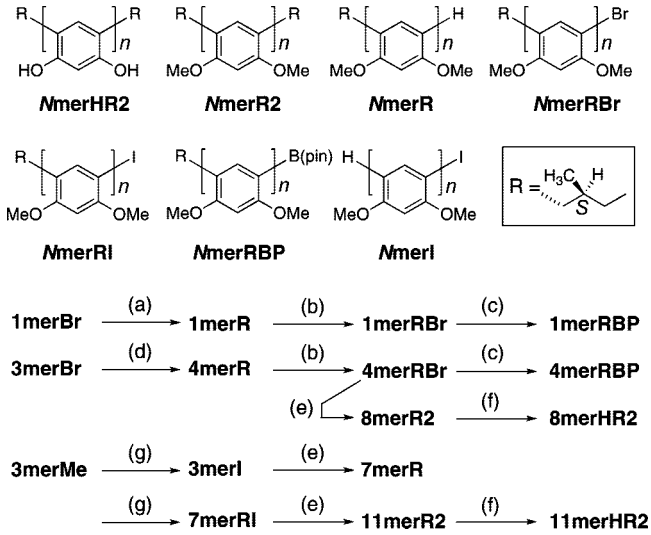

[a] Reagents and conditions: (a) (i) *t*-BuLi, THF, −78 °C, 25 min, (ii) $MgBr_2 \cdot Et_2O$, −78 °C, 30 min, (iii) (*S*)-1-bromo-2-methylbutane (RBr), $CuCl_2$, reflux, 2 days, (iv) H_3O^+; (b) DBH, THF, 0 °C, 1 day; (c) pinacolborane, $PdCl_2(PPh_3)_2$, NEt_3, 1,4-dioxane, 80 °C, 1 day; (d) **1merRBP**, $Pd(PPh_3)_4$, K_2CO_3, toluene H_2O, 80 °C, 3 days; (e) **4merRBP**, $Pd(PPh_3)_4$, K_2CO_3, toluene H_2O, 80 °C, 3 days; (f) BBr_3, 0 °C, 1 day; (g) 1,3-diiodo-5,5-dimethylhydantoin (DIH), THF, 0 °C, 1 day.

was introduced by the copper(II)-catalyzed coupling of the chiral bromide and the Grignard intermediate obtained by treatment of **1merBr** with *t*-BuLi and $MgBr_2 \cdot Et_2O$ to afford the chiral monomer (**1merR**).[18] The *O*-methyl-protected oligomers with the chiral side chains (**8merR2** and **11merR2**) were synthesized by the combination of bromination, conversion of the bromides to the boronates, and the Suzuki coupling in a stepwise manner similar to the preparation of **2merH**−**12merH** and **15merH**. **8merHR2** and **11merHR2** were characterized by ^{1}H-, ^{13}C NMR, and IR spectroscopies and mass spectrometry (see Supporting Information).

Double Helix Formation of Oligoresorcinols: Chain-Length Dependence. We previously reported that **9merH** formed a double-stranded helix in neutral water through interstrand aromatic interactions, whereas it took a single-stranded random-coiled conformation in organic solvents such as MeOH.[9a] A significant chain-length dependence was observed for the double helix formation of the oligoresorcinols; **3merH** adopted a single-stranded conformation both in water and in organic solvents, while **6merH** existed as a mixture of the double helix and the single-stranded species. We investigated the further details of the chain-length dependence of the double helix formation by employing the oligomers from **1merH** to **12merH** as well as **15merH**.

In general, the chemical shifts of aromatic protons in the ^{1}H NMR spectra undergo upfield shifts when located above another aromatic ring, because of the ring current effects, thus being often utilized as a powerful indicator for aromatic interactions. We measured the ^{1}H NMR spectra of the oligoresorcinols in neutral D_2O[19] and in CD_3OD (Figure 2A,B). Upfield shifts of the ^{1}H NMR signals of the aromatic protons were observed for the longer oligomers in D_2O. In addition, the exchange between the single strands and the double helices is so fast on the ^{1}H NMR time scale that a set of averaged signals between those of the single strands and the double helices was observed. For **1merH** through **3merH** in D_2O, the chemical shifts did not show any apparent upfield shift (Figure 2A,C). However, the signals abruptly shifted upfield by about 0.3−0.5 ppm as the chain length increased from 3 to 7, and remained unchanged for **7merH**−**12merH** and **15merH**, but with a significant broadening in D_2O. In CD_3OD, where the oligoresorcinols take a single-stranded random-coiled conformation, the chemical shifts of the signals hardly changed for all the oligomers (Figure 2B,C). The upfield shifts observed in neutral D_2O are consistent with the interstrand aromatic stacking in the double helices, whereas no aromatic stacking is possible for the single strand, as apparent from the molecular mechanics calculated structures of the double helix and the single strand of **9merH** (Figure 1B).[9a]

The hypochromicity provides additional evidence for the aromatic stacking (Figure 3A−E). In the absence of aromatic interactions, the molar absorptivity per unit around 290 nm (ε_{max}) should be almost constant regardless of the chain length. However, in CD_3OD, the ε_{max} exhibited a monotonic increase with the increasing chain length from **1merH** to **15merH** (Figure 3C−E), which arises from the elongated conjugation, as evidenced by the red shift of the maximum wavelength around 290 nm (λ_{max}) with an increase in the chain length. In contrast, for **3merH** through **8merH** in D_2O, the ε_{max} decreased with an increase in the chain length, resulting in an apparent hypochromicity for **4merH** through **15merH**, which unambiguously indicated the presence of significant aromatic interactions (Figure 3A,B,E).

Figure 3F shows the diffusion constants (D) and the hydrodynamic diameters (d_h) of the oligoresorcinols estimated by the diffusion-ordered ^{1}H NMR spectroscopy (DOSY) measurements.[20] Both the obtained D values of the oligomers in D_2O and CD_3OD decreased with the increasing chain length, being consistent with the molecular weights. Overall, the D values in D_2O were lower than those in CD_3OD, due to the higher viscosity of water,[21] because the diffusion constant is inversely proportional to the solvent viscosity. The d_h values were then calculated from the Einstein−Stokes equation[22] using the D values in D_2O and CD_3OD, resulting in almost the same values for those in D_2O and CD_3OD. These results indicated that the molecular sizes of the single strands did not change much upon forming the double-stranded helices, and the oligoresorcinols do not form any larger aggregates in the solvents.

Helix-Sense Bias Induction. Circular dichroism (CD) measurements along with absorption and ^{1}H NMR spectroscopic studies were carried out to investigate the helix-sense bias induction for the 8mer and 11mer with chiral side chains at both ends (**8merHR2** and **11merHR2**) (Figure 4). In CD_3OD, both oligomers existed as random-coiled single strands, as evidenced by the clear ^{1}H NMR spectra without upfield shifts nor broadening of the signals, whereas they adopted a double helical conformation in D_2O, exhibiting considerable upfield shifts as well as broadening of the ^{1}H NMR signals. As expected from the fact that the oligomers took a random coil conformation

(18) Terao, J.; Ikumi, A.; Kuniyasu, H.; Kambe, N. *J. Am. Chem. Soc.* **2003**, *125*, 5646–5647.
(19) Glasoe, P. K.; Long, F. A. *J. Phys. Chem.* **1960**, *64*, 188–190.
(20) For reviews on DOSY technique, see: (a) Cohen, Y.; Avram, L.; Frish, L. *Angew. Chem., Int. Ed.* **2005**, *44*, 520–554. (b) Pregosin, P. S.; Kumar, P. G. A.; Fernández, I. *Chem. Rev.* **2005**, *105*, 2977–2998.
(21) For the solvent viscosity values (η_0) of water and methanol, see: *CRC Handbook of Chemistry and Physics*, 84th ed.; Lide, D. R., Ed.; CRC Press: Boca Raton, FL, 2003−2004; pp **8**−69.
(22) $d_h = k_B T/3\pi\eta_0 D$ (k_B: Boltzmann constant; T: absolute temperature; η_0: solvent viscosity; D: diffusion constant).

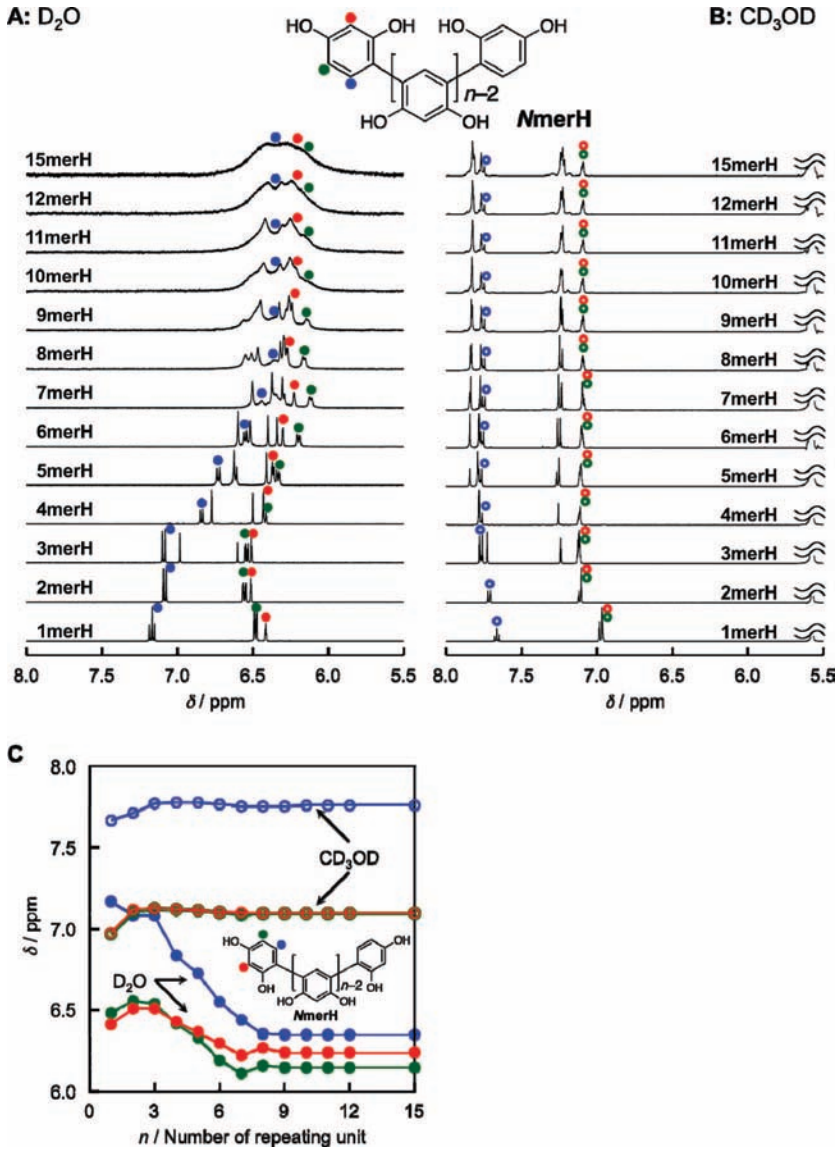

Figure 2. (A and B) ^{1}H NMR spectra of the oligoresorcinols (**1merH**−**12merH** and **15merH**) in D_2O (pD = 5.3) (A) and CD_3OD (B) at 25 °C. (C) Plots of the ^{1}H NMR chemical shifts of the terminal rings of the oligoresorcinols (**1merH**−**12merH** and **15merH**) versus number of repeating unit in D_2O (●) and CD_3OD (○) at 25 °C; [repeating unit of the oligoresorcinol] = 9 mM.

in CD_3OD, neither of them showed Cotton effects in the backbone chromophore regions in CD_3OD. In sharp contrast, the chiral oligomers exhibited remarkable Cotton effects in D_2O, indicating the helix-sense bias of the double helices caused by the chiral side chains at both ends. The quite similar CD patterns observed for the oligomers suggested that they virtually adopted the same double helical conformation with the same helix sense. The molar circular dichroism ($\Delta\varepsilon$) per unit of **8merHR2** in D_2O was ca. 1.5-fold higher than that of **11merHR2**, suggesting that the helix-sense bias is higher for **8merHR2** than for **11merHR2**. Thus, the (*S*)-2-methylbutyl chain is effective as a chiral director to produce a helix-sense bias of the double helices (for the effect of temperature on the helix-sense bias, see below).

Effect of pH. We next examined the pH effect on the double helix formation of the oligoresorcinols, which is likely to be significantly affected by pH, since they have the two acidic hydroxyl groups on each benzene ring. We employed the ^{1}H NMR and CD spectroscopies for this investigation, since absorption spectroscopy could hardly discriminate spectral changes due to the aromatic interactions from those caused by the protonation and deprotonation of the hydroxyl groups upon a pH change (Figures 5 and S1 in the Supporting Information). The chemical shifts of the protons at the 2-position on the middle rings of **3merH**, **9merH**, and **8merHR2** (δ_{mid}) as well as the $\Delta\varepsilon_{236}$ values of **8merHR2** in D_2O were plotted versus pD. An increase in the pD brought about slight downfield shifts in the signals of **3merH** around a pD of about 7−9, which is attributable to the deprotonation of the hydroxyl groups. On the other hand, upon raising the pD, significant downfield shifts were observed for the δ_{mid} of **9merH** and **8merHR2** with clear transition points at pD = 8.8 and 8.3, respectively, and the chemical shifts became almost the same as those of **3merH** above pD = 9. In addition, the CD intensities of **8merHR2** were drastically decreased with a clear transition point at pD = ca. 8.3, and **8merHR2** became almost CD-silent above pD = 9. These results indicate that both the double-stranded helices of **9merH** and **8merHR2** formed in D_2O below pH = 6 were unwound into the single strands due to the electrostatic repulsion

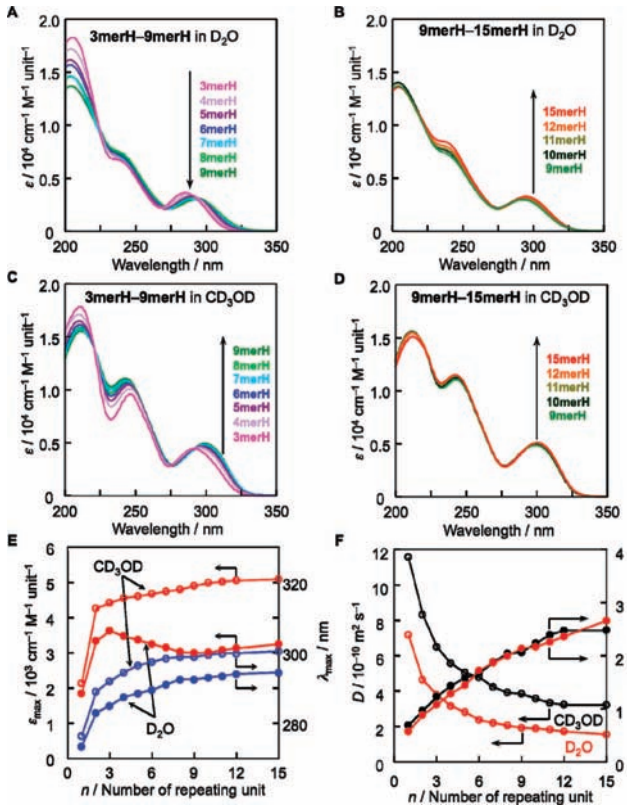

Figure 3. (A−D) Absorption spectra of the oligoresorcinols (**3merH**−**9merH** (A, C), and **9merH**−**12merH** and **15merH** (B, D)) in D_2O (pD = 5.3) (A and B) and CD_3OD (C and D) at 25 °C. (E) Plots of the maximal molar absorptivities per repeating unit (ε_{max}) and the wavelengths at the peak maxima (λ_{max}) around 300 nm (**1merH**−**12merH** and **15merH**) versus number of repeating unit in D_2O (●) and CD_3OD (○) at 25 °C; [repeating unit of the oligoresorcinol] = 9 mM. (F) Plots of the diffusion coefficients (D) (○) and the hydrodynamic diameters (d_h) (●) of oligoresorcinols (**1merH**−**12merH** and **15merH**) versus number of repeating units in D_2O (pD = 5.3) (red) and CD_3OD (black) at 25 °C; [repeating unit of oligoresorcinol] = 9 mM.

between the two negatively charged strands by the deprotonation of the hydroxyl groups at a high pH in D_2O.[23]

Effect of Temperature and Salt. The hyperchromicity upon dissociation of the oligoresorcinols' double helices into single strands is a powerful indicator of their stability, as already described. The double helix formation of the oligoresorcinols was further studied by changing the temperature, and the melting temperatures (T_m) from the measurements were assigned as the inflection points (Figure 6). Temperature-dependent absorption measurements in H_2O demonstrated that increasing the temperature of a solution of **6merH** in H_2O from −10 to 70 °C led to destabilization of the double helices as evidenced by the increasing absorbance at ca. 290 nm (Figure 6A,B).[9a] Thus, the double helix formation of the oligoresorcinols is mainly governed by the "nonclassical" hydrophobic effect (i.e., an enthalpy-driven process).[24] The T_m increased with the increasing chain length from **6merH** to **9merH** as well as by the addition of NaCl, indicating that the stabilization of the double helix of

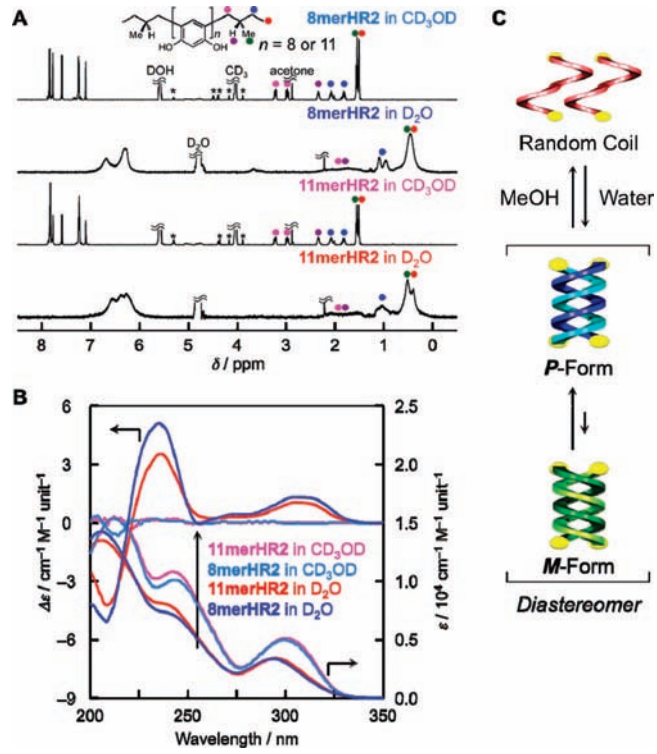

Figure 4. (A and B) ^1H NMR (A), CD, and absorption (B) spectra of **8merHR2** (blue and aqua) and **11merHR2** (red and pink) in D_2O (pD = 5.3) (blue and red) and CD_3OD (aqua and pink) at 25 °C; [repeating unit of oligoresorcinol] = 9 mM. Asterisks denote signals from the solvents and impurities. (C) Schematic illustration for the double-helix formation of **8merHR2** and **11merHR2** with an excess one-handed helix sense. The predominant helix sense of the double helices in the schematic illustration is tentative.

the oligoresorcinols resembles the nucleic acids of which the stability increases with the increasing chain length and salt concentration.[25]

The intense induced CD (ICD) spectra of the chiral oligomers (**8merHR2** and **11merHR2**) in H_2O are attributable to the helix-sense bias of the double helices caused by the chiral side chains at both ends, as already mentioned. The Cotton effect intensities gradually decreased with the increasing temperature and completely disappeared at ca. 80 °C (Figure 6C−F). The disappearance of the ICD indicates the formation of an equimolar mixture of the right- and left-handed double helices, since a majority of the oligomers remained as double helices at the temperature, as apparent from the UV melting curves. The Cotton effect intensities reversibly changed in quick response to the temperature, implying a very fast process for the interconversion between both helix senses. The addition of NaCl to the solutions of the chiral oligomers brought about a slight enhancement of the CD intensities of both oligomers, which reflected an increase in the helix-sense biases of the double helices (Figure 6E,F).

Association Constants for Double Helix Formation. The chain-length dependence of the stability of the oligoresorcinols was investigated in terms of the association constants (K_a) by ^1H NMR and absorption titrations (Figures 7 and S2 and S3 in the Supporting Information).[26] We examined the concentration dependence of the ^1H NMR spectra of **4merH** in the concentra-

(23) (a) Chung, J.; Deming, T. J. *Macromolecules* **2001**, *34*, 5169–5174. (b) Goto, H.; Furusho, Y.; Yashima, E. *Chem. Commun.*, in press. DOI: 10.1039/b900113a.

(24) (a) Ferguson, S. B.; Seward, E. M.; Diederich, F.; Sanford, E. M.; Chou, A.; Inocencio-Szweda, P.; Knobler, C. B. *J. Org. Chem.* **1988**, *53*, 5595–5596. (b) Meyer, E. A.; Castellano, R. K.; Diederich, F. *Angew. Chem., Int. Ed.* **2003**, *41*, 1210–1250.

(25) Saenger, W. Forces stabilizing associations between bases: Hydrogen bonding and base stacking. In *Principles of Nucleic Acid Structure*; Springer-Verlag: New York, 1984; Chapter 6, pp 116−158.

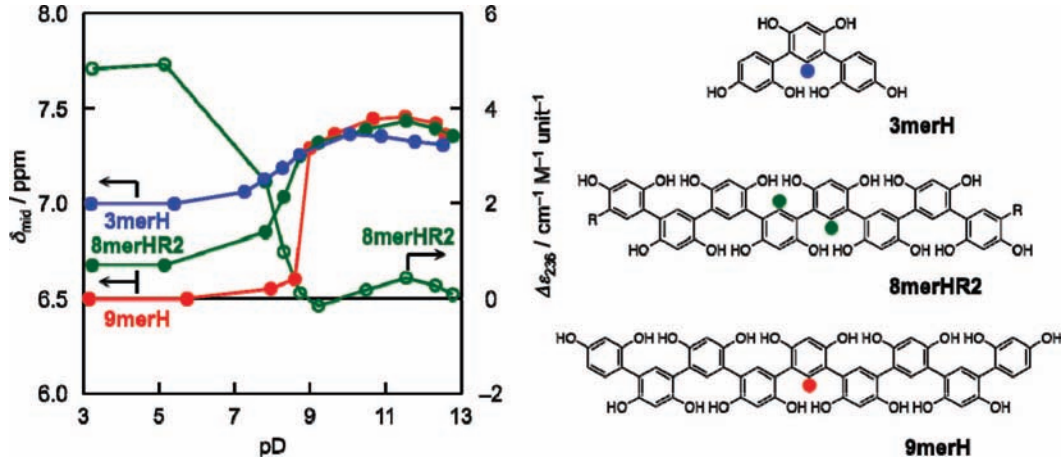

Figure 5. Plots of the chemical shifts (δ_{mid}) of the protons at the 2-position in the middle benzene rings (●) of **3merH**, **9merH**, and **8merHR2** and the $\Delta\varepsilon_{236}$ values (○) of **8merHR2** versus pD in D_2O at 25 °C; [repeating unit of oligoresorcinol] = 4.5 mM.

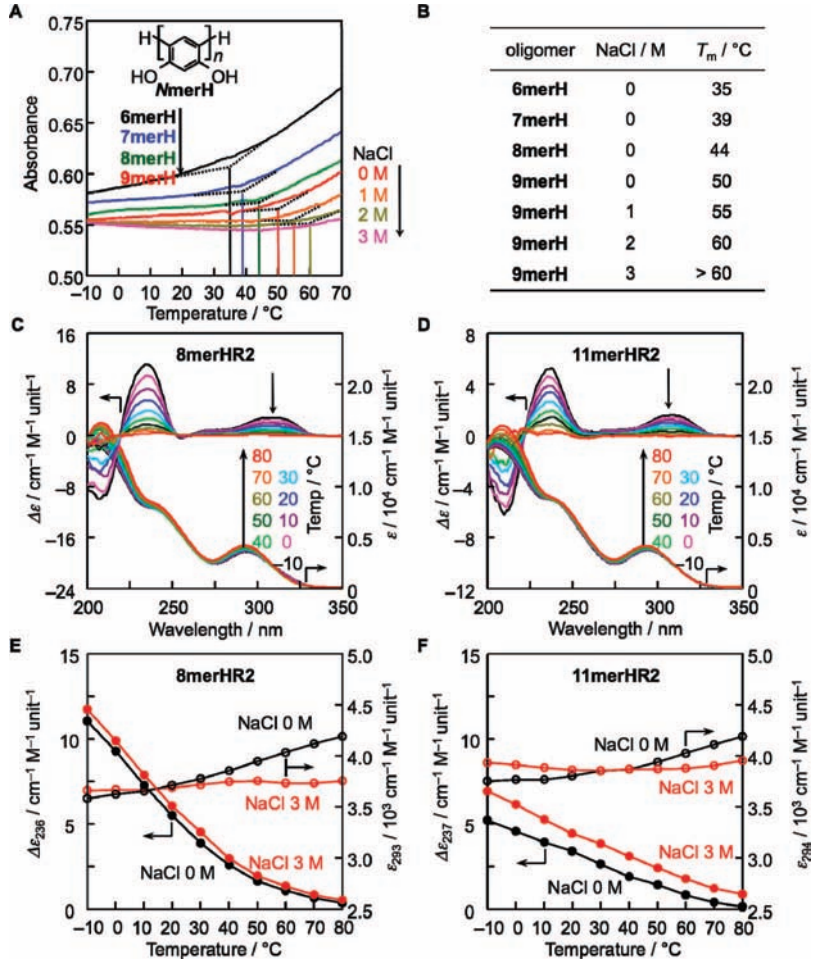

oligomer	NaCl / M	T_m / °C
6merH	0	35
7merH	0	39
8merH	0	44
9merH	0	50
9merH	1	55
9merH	2	60
9merH	3	> 60

Figure 6. (A) Melting curves of **6merH**−**9merH** in H_2O with NaCl (0−3 M); λ = 290−293 nm; pH = 4.8−5.3; heating rate = 0.5 °C/min. (B) Lists of the melting temperatures of **6merH**−**9merH**. (C, D) CD and absorption spectra of **8merHR2** (C) and **11merHR2** (D) in H_2O at various temperatures. (E, F) Plots of $\Delta\varepsilon_{second}$ and ε of **8merHR2** (E) and **11merHR2** (F) versus temperature; [repeating unit of oligoresorcinol] = 1.8 mM.

tion range from 0.016 to 64 mM in D_2O (Figure 7A). Upon dilution, the chemical shifts of the protons at the 2-position of the two middle rings shifted downfield, which reflected the dissociation into single strands. The K_a for **4merH** was calculated to be (3.5 ± 0.1) × 10^2 M^{-1} at 25 °C from the nonlinear least-squares curve fitting of the data.[27] The dilution experiments for oligomers longer than **4merH** were carried out by absorption spectroscopy, since their association constants

(26) Connors, K. A. *Binding Constants: The Measurement of Molecular Complex Stability*; Wiley & Sons: New York, 1987.

(27) The observed shifts (δ_{obs}) were fit to the equation $\delta_{obs} = \delta_{dimer} + (\delta_{monomer}-\delta_{dimer})[\{-1 + (1 + 8K_aC)^{1/2}\}/(4K_aC)]$, where C corresponds to the total concentration of the oligoresorcinol and $\delta_{monomer}$ and δ_{dimer} are the chemical shifts of the monomer and the dimer, respectively.

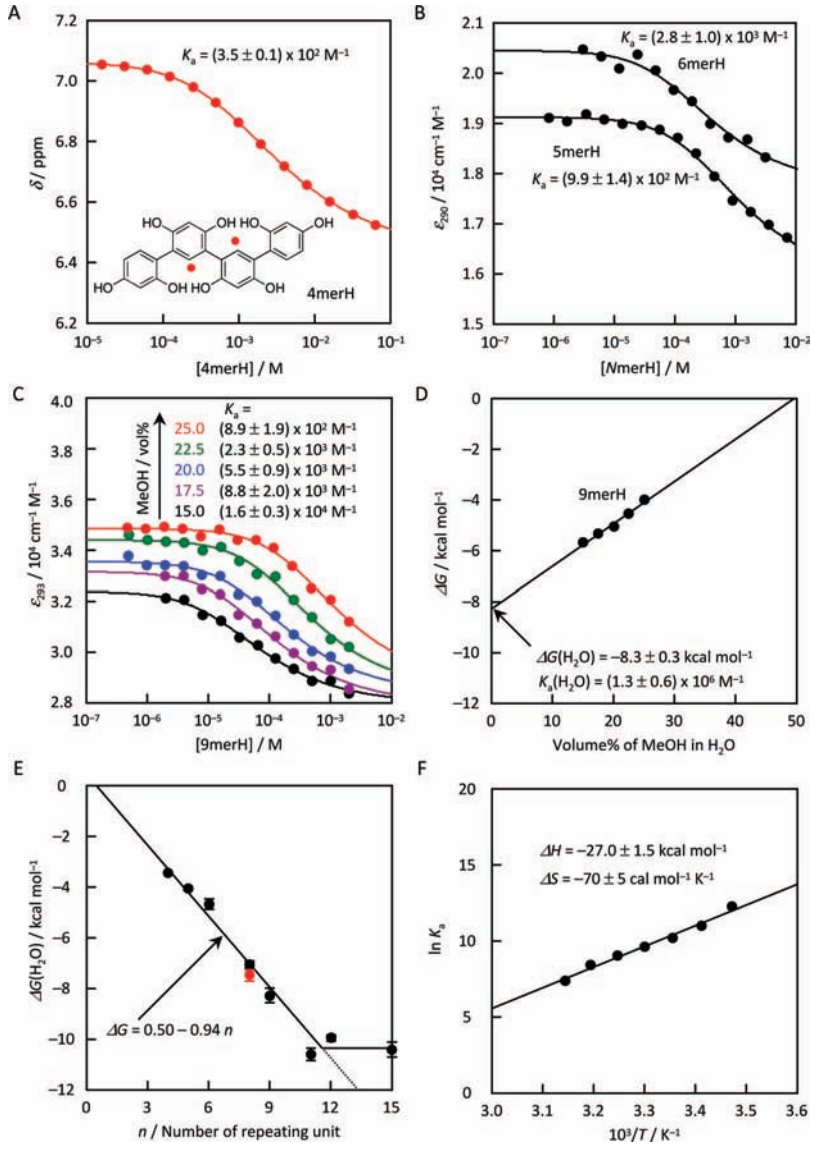

Figure 7. (A) Plots of the chemical shifts of the protons at the 2-position on the middle rings of **4merH** (δ) versus the logarithm of the concentrations in D_2O. (B) Plots of the ε_{290} values of **5merH** and **6merH** versus the logarithm of the concentrations in H_2O. (C) Plots of the ε_{293} values versus the logarithm of the concentrations of **9merH** in various H_2O/MeOH mixtures (pH = 4.8−5.3) at ca. 23 °C; [**9merH**] = 0.0005−2 mM. (D) Plots of ΔG of **9merH** versus vol % of MeOH in H_2O. (E) Plots of ΔG (H_2O) versus the number of the repeating units of various oligoresorcinols (**4**−**6merH**, **8merH**, **8merHR2** (red), **9merH**, **11merH**, **12merH**, and **15merH**). (F) The van't Hoff plot for the double helix formation of **9merH** in H_2O/MeOH (80/20, v/v, pH = 5.0) over a temperature range of 10−45 °C; [**9merH**] = 0.0078−0.5 mM. The solid curves represent the curve fittings.

were higher than those suitable to ^{1}H NMR spectroscopy. The data obtained from the dilution titrations gave the K_a values of (9.9 ± 1.4) × 10^2 and (2.8 ± 1.0) × 10^3 M^{-1} for **5merH** and **6merH** in D_2O, respectively (Figure 7B), on the basis of the nonlinear curve fitting.[28]

For the oligomers longer than **6merH** such as **9merH**, we estimated the K_a values in the mixed solvents of H_2O/MeOH at 25 °C, since the association constants in H_2O were so high that the hyperchromicities did not reach the midpoints even at concentrations as low as 10^{-7} M (i.e., the detection limit for our spectrophotometer with a 10-cm quartz cell). Figure 7C shows the dilution titration data of the molar absorptivities of **9merH** in several H_2O/MeOH mixtures (from 85/15 to 75/25, v/v). The K_a values decreased as the volume ratio of MeOH increased: K_a = (1.6 ± 0.3) × 10^4 M^{-1} (15.0 vol % MeOH); (8.8 ± 2.0) × 10^3 M^{-1} (17.5 vol % MeOH); (5.5 ± 0.9) × 10^3 M^{-1} (20.0 vol % MeOH); (2.3 ± 0.5) × 10^3 M^{-1} (22.5 vol % MeOH); (8.9 ± 1.9) × 10^2 M^{-1} (25.0 vol % MeOH). The corresponding free energy changes (ΔG) were then calculated by the standard relationship, $\Delta G = -RT \ln K_a$, where R is the gas constant and T is the absolute temperature, and plotted versus the solvent composition as shown in Figure 7D, which suggested a linear relationship between the free energy changes and the solvent composition.[29] By extrapolating the data to the y-intercept using the least-squares curve fitting method, the free

(28) The observed molar absorptivities (ε_{obs}) were fit to the equation $\varepsilon_{obs} = \varepsilon_{dimer}/2 + (\varepsilon_{monomer} - \varepsilon_{dimer}/2)[\{-1 + (1 + 8K_aC)^{1/2}\}/(4K_aC)]$, where C corresponds to the total concentration of the oligoresorcinol and $\varepsilon_{monomer}$ and ε_{dimer} are the molar absorptivities of the monomer and dimer, respectively.

(29) Prince, R. B.; Saven, J. G.; Wolynes, P. G.; Moore, J. S. *J. Am. Chem. Soc.* **1999**, *121*, 3114–3121.

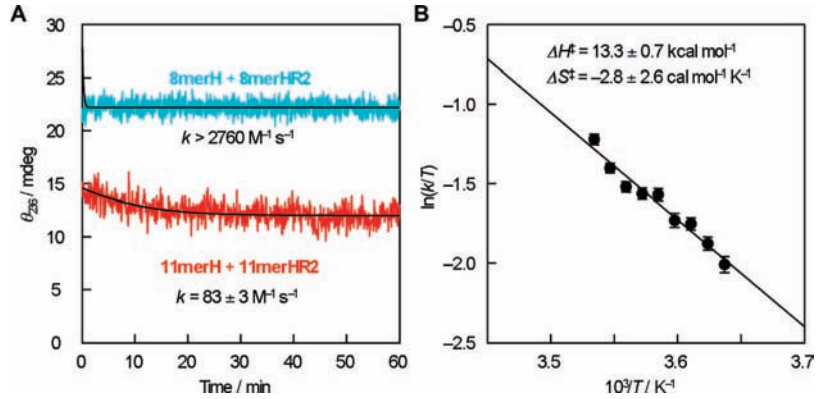

Figure 8. (A) Changes of the CD intensities (θ_{236}) of (**8merHR2**)$_2$ (aqua) and (**11merHR2**)$_2$ (red) in 4 M NaCl−H_2O at 10 °C after the addition of **8merH** and **11merH**, respectively, versus time; [**8merH**] = [**8merHR2**] = 11.3 μM, [**11merH**] = [**11merHR2**] = 8.2 μM, cell length = 1 cm. The black curves represent the curve fitting results. (B) Eyring plot for the chain exchange reaction over a temperature range of 2−10 °C.

energy change in pure water was estimated to be -8.3 ± 0.3 kcal mol^{-1}, which corresponds to the K_a of $(1.3 \pm 0.6) \times 10^6$ M^{-1}.

The K_a values of other oligomers in H_2O were also estimated in a similar fashion: $(1.6 \pm 0.4) \times 10^5$ M^{-1} for **8merH**; $(6.6 \pm 2.7) \times 10^7$ M^{-1} for **11merH**; $(2.2 \pm 0.4) \times 10^7$ M^{-1} for **12merH**; $(4.8 \pm 2.5) \times 10^7$ M^{-1} for **15merH** (Figures S2 and S3 in the Supporting Information). The introduction of the chiral side chains did not significantly affect the association constants; the K_a for **8merHR2** was estimated to be $(3.3 \pm 1.2) \times 10^5$ M^{-1}, slightly higher than that for **8merH**, $K_a = (1.6 \pm 0.4) \times 10^5$ M^{-1} with a difference in a $\Delta\Delta G$ of 0.43 kcal mol^{-1}. The free energy changes were calculated from the K_a values and plotted versus the number of repeating units (Figure 7E). The free energy changes linearly decreased with the slope of −0.94 kcal mol^{-1} unit^{-1} from **4merH** to **11merH**, comparable to the ΔG change per base pair of the double-stranded helix formation of DNA in H_2O with NaCl (1 M) at 37 °C (ca. −1.2 kcal mol^{-1} bp^{-1}).[30] However, further growth of the chain length ($n \geq 12$) resulted in almost no ΔG change, suggesting that, above the 12mer, the enthalpic gain by the increase in the aromatic rings may be offset by the entropic loss due to the reduced mobility of the strands, which is supported by the considerable broadening of the ^{1}H NMR spectra of the higher oligomers.[31]

To study the temperature dependence of the double helix formation, the changes in the K_a of **9merH** in H_2O/MeOH (80/20, v/v) at 10−45 °C were measured by absorption titrations (Figures 7F and S4 in the Supporting Information). The van't Hoff plot provided the corresponding thermodynamic parameters of $\Delta H = -27.0 \pm 1.5$ kcal mol^{-1} and $\Delta S = -70 \pm 5$ cal mol^{-1} K^{-1}. Accordingly, the double helix formation is an enthalpically driven process,[24] quite similar to those observed for the heterodouble helix formation of **9merH** with *linear* oligosaccharides.[9c]

Kinetic Study of Chain Exchange Reaction. Upon mixing of equimolar amounts of (**8merH**)$_2$ and (**8merHR2**)$_2$ or (**11merH**)$_2$ and (**11merHR2**)$_2$ in H_2O, the two different strands with the same chain length hybridized to form the corresponding heterodouble helix through the chain exchange process, as confirmed by MALDI-TOF mass spectrometry (Figures S5 and S6 in the Supporting Information).[32] The CD spectra of the mixtures were different from those simulated for the equimolar mixtures of the homodouble helices, also supporting the formation of the heterodouble helices through hybridization (Figure S7 in the Supporting Information). With the aim of elucidating the mechanism of the chain exchange process between the two different homodouble helices of the oligoresorcinols in H_2O, the kinetics of the chain exchange was investigated using CD spectroscopy (Figures 8 and S8 in the Supporting Information). Figure 8A shows the changes in the CD intensities of the **8merH/8merHR2** and **11merH/11merHR2** mixtures at 236 nm (the second Cotton effect with a positive sign) in H_2O and NaCl (4 M) at 10 °C versus time. As soon as (**8merH**)$_2$ was mixed with (**8merHR2**)$_2$ in H_2O with NaCl (4 M), the mixture reached an equilibrium within 1 min and no detectable CD change was observed for 1 h thereafter, resulting from a very fast chain exchange process. In contrast, upon the addition of (**11merH**)$_2$ to a (**11merHR2**)$_2$ solution, the mixture showed a gradual decrease in the θ_{236} value derived from the formation of the heterodouble helix, **11merH·11merHR2**. The rate of the chain exchange process (k) was estimated by treating it as a second-order reversible reaction (eq 1) with the nonlinear least-squares curve fitting of the CD changes (Figures 8 and S8 and Table S1 in the Supporting Information):[33]

(30) (a) Privalov, P. L.; Ptitsyn, O. B. *Biopolymers* **1969**, *8*, 559–571. (b) Pohl, F. M. *Eur. J. Biochem.* **1974**, *42*, 495–504. (c) SantaLucia, J. *Proc. Natl. Acad. Sci. U.S.A.* **1998**, *95*, 1460–1465.

(31) Negative length dependence was observed for duplex formation of oligo(aminotriazine)s and helix formation of oligoalanines. (a) Archer, E. A.; Krische, M. J. *J. Am. Chem. Soc.* **2002**, *124*, 5074–5083. (b) Job, G. E.; Kennedy, R. J.; Heitmann, B.; Miller, J. S.; Walker, S. M.; Lemp, D. S. *J. Am. Chem. Soc.* **2006**, *128*, 8227–8233.

(32) In general, the quantitative performance of MALDI-TOF-MS is not sufficient because of variability in the ionization potentials for different compounds. However, some groups recently used MALDI-TOF-MS for quantitative analyses of noncovalent assemblies of proteins and saccharides. In our case, it is reasonable to assume that the ionization potentials for the homo- and heterodouble helices with the same chain lengths are almost the same, because their chemical structures are quite similar to each other except for the chiral oligomers that possess chiral alkyl groups at both ends of the strands. (a) Jespersen, S.; Niessen, W. M. A.; Tjaden, U. R.; van der Greef, J. *J. Mass Spectrom.* **1995**, *30*, 357–64. (b) Mirgorodskaya, O. A.; Kozmin, Y. P.; Titov, M. I.; Korner, R.; Sonksen, C. P.; Roepstorff, P. *Rapid Commun. Mass Spectrom.* **2000**, *14*, 1226–1232. (c) Bucknall, M.; Fung, K. Y. C.; Duncan, M. W. *J. Am. Soc. Mass Spectrom.* **2002**, *13*, 1015–1027. (d) Nedelkov, D.; Nelson, R. W.; Kiernan, U. A.; Niederkofler, E. E.; Tubbs, K. A. *FEBS Lett.* **2003**, *536*, 130–134. (e) Nishimura, S.-I.; Niikura, K.; Kurogochi, M.; Matsushita, T.; Fumoto, M.; Hinou, H.; Kamitani, R.; Nakagawa, H.; Deguchi, K.; Miura, N.; Monde, K.; Kondo, H. *Angew. Chem., Int. Ed.* **2005**, *44*, 91–96.

$$(\mathbf{11merHR2})_2 + (\mathbf{11merH})_2 \underset{k_-}{\overset{k}{\rightleftharpoons}} 2 \times (\mathbf{11merH{\cdot}11merHR2})_2 \quad (1)$$

The reaction rate for the **11merH/11merHR2** mixture was then estimated to be $k = 83 \pm 3\ M^{-1}\ s^{-1}$ at 10 °C. The k values of the **11merH/11merHR2** (1/1) mixture at various temperatures were calculated in the same fashion as already described, resulting in a gradual increase in the k values with increasing temperature (Table S1 in the Supporting Information). The activation parameters ($\Delta H^{\ddagger}$ and $\Delta S^{\ddagger}$) of the chain exchange process were then estimated to be 13.3 ± 0.7 kcal mol^{-1} and -2.8 ± 2.6 cal mol^{-1} K^{-1}, respectively, on the basis of the Eyring plot of the data (Figure 8B). Considering the small $\Delta S^{\ddagger}$ for the intermolecular chain exchange as well as the high K_a values for the double helix formation of the oligoresorcinols, the chain exchange is likely to proceed not via a dissociation−exchange pathway (Figure 9, route B), but via a direct exchange one (Figure 9, route A).

Conclusions

We disclosed in this study that the double helix formation of the oligoresorcinols in water has a remarkable dependence on the chain length and is also significantly affected by external conditions, such as the solvent, pH, salt, and temperature. The free energy change for the double helix formation ($-\Delta G$) linearly increases with the increasing chain length from **4merH** to **11merH**, whereas it did not change for the oligomers longer than **11merH**. The van't Hoff analysis of **9merH** revealed that the double helix formation is an enthalpically driven process, which is consistent with the upfield shifts in the ^{1}H NMR spectra and the hypochromic effect of the absorption spectra, indicating the interstrand aromatic interactions in water. The kinetic analysis of the chain exchange reaction showed that it is a quite fast process with a small $\Delta S^{\ddagger}$ value, which suggests that the chain exchange reaction proceeds not via a dissociation-exchange pathway, but via a direct exchange one. These comprehensive mechanistic, thermodynamic, and kinetic studies on the double helix formation of the oligoresorcinols provide not only insight into the principle underlying the generation of double helical conformations in water, but also a clue for the development of novel water-soluble, supramolecular assemblies with electronic and biological functions based on the oligo- and poly(*m*-phenylene) backbones.[34] Work along this line is currently ongoing in our laboratory.

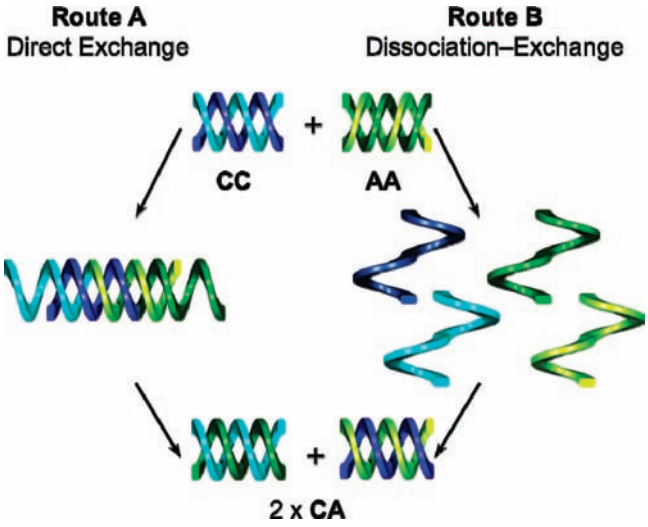

Figure 9. Illustration of possible mechanisms (routes A and B) of the chain exchange between the homodouble helices composed of chiral (C) and achiral (A) strands.

Acknowledgment. This work was supported in part by Grant-in-Aid for Scientific Research from the Japan Society for the Promotion of Science (JSPS) and Japan Science and Technology Agency (JST). We thank Mr. Toshihide Hasegawa (JST) for his help in the synthesis of the oligoresorcinols.

Supporting Information Available: Full experimental details in the characterization of the oligoresorcinols. This material is available free of charge via the Internet at http://pubs.acs.org.

JA808585Y

(33) (a) Moriyasu, M.; Hashimoto, Y. *Bull. Chem. Soc. Jpn.* **1980**, *53*, 3590–3595. (b) Stach, J.; Kirmse, R.; Dietzsch, W.; Lassmann, G.; Belyaeva, V. K.; Marov, I. N. *Inorg. Chim. Acta* **1985**, *96*, 55. (c) Habermehl, N. C.; Angus, P. M.; Kilah, N. L.; Norén, L.; Rae, A. D.; Willis, A. C.; Wild, S. B. *Inorg. Chem.* **2006**, *45*, 1445–1462.

(34) (a) Yamamoto, T.; Hayashi, Y.; Yamamoto, A. *Bull. Chem. Soc. Jpn.* **1978**, *51*, 2091–2097. (b) Musfeldt, J. L.; Reynolds, J. R.; Tanner, D. B.; Ruiz, J. P.; Wang, J.; Pomerantz, M. *J. Polym. Sci., Part B: Polym. Phys.* **1994**, *32*, 2395–2404. (c) Kang, B. S.; Seo, M.-L.; Jun, Y. S.; Lee, C. K.; Shin, S. C. *Chem. Commun.* **1996**, 1167–1168. (d) Reddinger, J. L.; Reynolds, J. R. *Macromolecules* **1997**, *30*, 479–481. (e) Panda, M.; Chandrasekhar, J. *J. Am. Chem. Soc.* **1998**, *120*, 13517–13518. (f) Mandal, B. K.; Walsh, C. J.; Sooksimuang, T.; Behroozi, S. J. *Chem. Mater.* **2000**, *12*, 6–8. (g) Yamamoto, T.; Abe, M.; Wu, B.; Choi, B.-K.; Harada, Y.; Takahashi, Y.; Kawata, K.; Sasaki, S.; Kubota, K. *Macromolecules* **2007**, *40*, 5504–5512. (h) Rager, T.; Schuster, M.; Steininger, H.; Kreuer, K.-D. *Adv. Mater.* **2007**, *19*, 3317–3321.